# Analysis of the temporal expression of chemokines and chemokine receptors during experimental granulomatous inflammation: role and expression of MIP-1α and MCP-1

[1]Maria Carollo, [2]Cory M. Hogaboam, [2]Stephen L. Kunkel, [3]Stephen Delaney, [3]Mark I. Christie & *,[1]Mauro Perretti

[1]William Harvey Research Institute, Pharmacology Division, St. Bartholomew's and The Royal London School of Medicine and Dentistry, Charterhouse Square, London, EC1M 6BQ; [2]Department of Pathology, University of Michigan Medical School, Ann Arbor, Michigan, MI 48109-0602, U.S.A. and [3]AstraZeneca R&D, Charnwood, Loughborough, Leics LE11 5RH

**1**  Chemokine expression and function was monitored in an experimental model of granulomatous tissue formation after injection of croton oil in complete Freund's adjuvant (CO/CFA) into mouse dorsal air-pouches up to 28 days.

**2**  In the first week, mast cell degranulation and leukocyte influx (mononuclear cell, MNC, and polymorphonuclear cell, PMN) were associated with CXCR2, KC and macrophage inflammatory protein (MIP)-2 mRNA expression, as determined by TaqMan® reverse transcriptase-polymerase chain reaction. KC ($\sim$400 pg mg protein$^{-1}$, $n=12$) and MIP-2 ($\sim$800 pg mg protein$^{-1}$, $n=12$) proteins peaked at day 7, together with myeloperoxidase (MPO) activity. Highest MIP-1α ($>1$ ng mg protein$^{-1}$, $n=12$) levels were measured at day 3.

**3**  After day 7, a gradual increase in CCR2 and CCR5 mRNA, monocyte chemoattractant protein (MCP)-1 mRNA and protein expression was measured. MCP-1 protein peaked at day 21 ($\sim$150 pg mg protein$^{-1}$, $n=12$) and was predominantly expressed by mast cells. A gradual increase in N-acetyl-$\beta$-D-glucosaminidase (NAG) activity (maximal at 28 days) was also measured.

**4**  An antiserum against MIP-1α did not modify the inflammatory response measured at day 7 (except for a 50% reduction in MIP-1α levels), but provoked a significant increase in MPO, NAG and MCP-1 levels as measured at day 21 ($n=6$, $P<0.05$). An antiserum to MCP-1 reduced NAG activity at day 21 but increased MPO activity values ($n=8$, $P<0.05$).

**5**  In conclusion, we have shown that CO/CFA initiates a complex inflammatory reaction in which initial expression of MIP-1α serves a protective role whereas delayed expression of MCP-1 seems to have a genuine pro-inflammatory role.
*British Journal of Pharmacology* (2001) **134**, 1166–1179

## Introduction

The initial phases of the host inflammatory response are characterized by the synthesis and release of several soluble mediators both peptidic and non-peptidic in nature. In particular, multi-potent cytokines such as interferon-γ, interleukin (IL)-1, IL-4 or tumour necrosis factor (TNF)-α activate cells adjacent to the site of injury, including resident leukocytes (macrophages and mast cells), endothelial cells and interstitial fibroblasts (Smith *et al.*, 1997; Paul & Seder, 1994). Chemotactic factors are then generated to promote extravasation of blood-borne leukocytes (Gao *et al.*, 1997; Luster, 1998). Amongst the latter group of mediators, an important role is occupied by chemokines.

Chemokines are low molecular weight proteins classified according to the presence or absence of an amino acid between the first two cysteines, yielding CXC chemokines and CC chemokines (Baggiolini, 1998), or CXCL and CCL chemokines according to a more recent nomenclature (Zlotnik & Yoshie, 2000). CXC chemokines act predominantly on neutrophils and T lymphocytes, whereas CC chemokines are able to chemoattract monocytes, T lymphocytes, eosinophils, basophils, dendritic cells and NK cells, depending on the specific protein (Mantovani, 1999). In the mouse, examples of CXC chemokines are KC (CXCL1) and macrophage inflammatory protein (MIP)-2 (CXCL2), whereas monocyte chemoattractant protein (MCP)-1 (or CCL2), MIP-1α (or CCL3), regulated on activated normal T cell expressed and secreted (RANTES or CCL5) and eotaxin (CCL11) belong to the CC chemokine group (Furie & Randolph, 1995; Luster, 1998). The distinction among the

*Author for correspondence; E-mail: M.Perretti@qmw.ac.uk

chemokine sub-groups is maintained also with respect to the receptor(s) they activate on target cells. CXCR are activated by CXC chemokines with a certain degree of promiscuity. CCR also share more than one chemokine (Premack & Schall, 1996; Zlotnik & Yoshie, 2000). For instance, CXCR2 can be activated by KC, MIP-2 or LPS-induced CXC chemokine (LIX or CXCL5), whereas CCR5 binds MIP-1β (CCL4) and RANTES with comparable affinities (Premack & Schall, 1996; Murphy *et al.*, 2000).

The specificity of chemokine actions suggests a key role in the co-ordination of a range of inflammatory responses. The expression and biological actions of a given chemokine provides a rationale for the predominance of distinct leukocyte subsets in different inflammatory pathologies and the development of selective chemokine receptor antagonists is a rational approach for the discovery of novel anti-inflammatory molecules (Murphy *et al.*, 2000). This line of research may lead to novel therapies for asthma, characterized by eosinophil influx, as well as rheumatoid arthritis, where neutrophil influx into the affected joint occurs during the acute phases of the disease (Kunkel *et al.*, 1996; Ward, 1997).

Few studies have investigated chemokine roles in long term models of chronic inflammation. For instance, the expression of MIP-2 and MIP-1α in a murine model of arthritis has been reported to be associated with development of the disease (Kasama *et al.*, 1995). A more recent study has investigated the time-dependency of mRNA expression for several chemokines in the model of collagen-induced arthritis (Thornton *et al.*, 1999). In a separate study, MCP-1 has been shown to have a central role in models of lung granuloma, with a preference towards those driven by a Th2 lymphocyte response (Chensue *et al.*, 1996).

In the present study we have used a model of murine granulomatous inflammation. Injection of a mixture of croton oil in complete Freund's adjuvant (CO/CFA) into a preformed dorsal air-pouch induces an intense inflammatory reaction associated with granuloma formation (Kimura *et al.*, 1985; 1986). A putative 'inflammatory phase' characterized by neutrophil influx and expression of pro-inflammatory cytokines such as IL-1α, IL-1β and tumour necrosis factor-α occurs within the first week of inflammation (Appleton *et al.*, 1993). This is followed by a putative 'repair phase' characterized by expression of anti-inflammatory cytokines (e.g. transforming growth factor-β) and occurs from day 14 onwards (Appleton *et al.*, 1993). We have used this model to investigate the expression of selected CXC and CC chemokines and chemokine receptors, at the level of transcription and translation, together with quantification of the recruitment of distinct cell types during the different stages of the inflammatory reaction. A neutralizing strategy has been used to address the specific role that the chemokine MIP-1α and MCP-1 may be playing in the context of this complex inflammatory reaction.

A succinct account of this work has been presented at two recent meetings of the British Pharmacological Society (Carollo *et al.*, 1999; 2000).

# Methods

## Animals

Female Swiss Albino mice (28–30 g body weight) were purchased from Banton and Kingsman (Hull, U.K.) and maintained on a standard chow pellet diet with tap water *ad libitum*. Animals were grouped at eight per cage in a room with controlled lighting (lights on 0800 h, off 2000 h) and temperature (21–23°C), and used 2–3 days after their arrival. Animal work was performed according to Home Office regulations (guidance on the operation of the Animals, (Scientific Procedures) Act 1986, United Kingdom).

## Chronic granulomatous inflammation

The granulomatous air-pouch model was performed as described in the studies by Kimura *et al.* (1995; 1986) and Appleton *et al.* (1993). Briefly, air pouches were formed by sub-cutaneous (s.c.) injection of 3 ml of air into the dorsal subcutaneous tissue. After 24 h (day 0), inflammation was induced by injection of 0.5 ml of 0.1% v v$^{-1}$ croton oil in complete Freund's adjuvant containing 5 mg ml$^{-1}$ *Mycobacterium tuberculosis* (CO/CFA) (Sigma-Aldrich Company Ltd, Poole, Dorset, U.K.) (Kimura *et al.*, 1985; 1986; Appleton *et al.*, 1993; Colville-Nash *et al.*, 1995). In some cases, 0.5 ml of incomplete Freund's adjuvant (IFA) alone were injected (Sigma-Aldrich) as a negative control group. A group of untreated animals was also added. At several days post-injection (days 3, 7, 14, 21, and 28), animals were sacrificed by CO$_2$ exposure and the whole air-pouches removed. The upper part of the granuloma was dissected together with the skin and used for histology (see below). The lower part of the granuloma was divided into three fragments, snap frozen and stored at −80°C prior to biochemical determinations (see below). In a few cases, the whole lower part of the granuloma was collected and its wet weight determined. Previous studies have demonstrated that the biochemical and histological characteristics of the upper and lower parts of the granuloma are identical (Appleton *et al.*, 1993).

## Preparation and analysis of tissue sections by histology

The skin and granuloma samples (upper part) were divided into three portions and fixed with different procedures specific for cryostat, paraffin or historesin sections.

*Cryostat sections*   Tissues were snap-frozen in cold isopentane (BDH Laboratory Supplies, Poole, Dorset, U.K.), fixed in O.C.T. compound (BDH Laboratory Supplies), and 10 μm sections cut in a cryostat, mounted on 3-aminopropyl-triethoxy-silane coated slides (BDH Laboratory Supplies) and stored at room temperature.

*Paraffin sections*   Tissue samples were fixed in 3% paraformaldehyde and 0.5% glutaraldehyde (TAAB Laboratories, Aldermaston, Berkshire, U.K.) in sodium cacodylate buffer (pH 7.4) for 24 h. Tissues were embedded in paraffin and 3 μm sections cut on an ultramicrotome (Reichert Ultracut; Leica, Austria), thereafter dewaxed with xylene and rehydrated through graded concentrations of ethanol.

*Historesin sections*   Following fixation in 3% paraformaldehyde and 0.5% glutaraldehyde (TAAB Laboratories), in sodium cacodylate buffer (pH 7.4) for 24 h, and embedding in historesin (Technovit 7200, Unicryl™, TAAB Laboratories), 1.5 μm sections were made and stained with May-

Grumwald (1:2) and Giemsa (1:10) (BDH Laboratory Supplies).

## Immunohistochemistry

Cryostat and paraffin sections were fixed in acetone and re-hydrated in 10 mM phosphate-buffered saline (PBS, pH 6.0). Endogenous peroxidases were quenched with 1% $H_2O_2$ (30% v $v^{-1}$) in methanol, prior to blocking non-specific binding with normal goat serum (Vectastain® ABC Kit, Vector Laboratories, Bretton, Peterbourough, U.K.) diluted 1:50 in PBS supplemented with 0.1% BSA (Sigma-Aldrich). Sections were incubated overnight at 4°C with a polyclonal rabbit anti-mouse MIP-1α (final dilution of 1:2000) or a polyclonal rabbit anti-mouse MCP-1 (final dilution of 1:1000), respectively. Both antibodies have been produced at the University of Michigan Medical School, and have been previously used to monitor the expression of these chemokines in murine models of inflammation (Chensue *et al.*, 1996; DiPietro *et al.*, 1998; Kunkel *et al.*, 1996; Standiford *et al.*, 1995). A non-immune rabbit serum (Sigma-Aldrich) was used as a negative control. Another control was represented by the anti-MCP-1 serum pre-absorbed (24 h, 4°C) with 1 μg mouse MCP-1 (R&D Systems, Abingdon, Oxon, U.K.). In all cases, tissues were counter-stained with 0.25% toluidine blue in 0.25% Michaelis' veronal acetate-hydrochloric acid buffer (pH 4.5) or Harris' haematoxylin (BDH Laboratory Supplies). Sections were air-dried and mounted in DPX (BDH Laboratory Supplies) prior to observation by light microscopy using an Olympus BH-2-RFCA microscope. The anti-MIP-1α antibody did not react with paraffin sections, whereas the anti-MCP-1 antibody reacted with both cryostat and paraffin sections.

## Semi-quantitative analysis of cell influx by histology

Historesin sections were used for morphological analysis of tissues obtained from IFA treatment and to determine cell number in granuloma tissues (after injection of CO/CFA) throughout the entire time course. Using a high power objective (magnification, ×600) cells were counted in three areas of approximately 100 $\mu m^2$, using five distinct serial sections (15 μm of space between each section) for two different animals by an observer unaware of the treatments. The degree of PMN ($\geq$90% neutrophils) and MNC (lymphocytes and monocytes/macrophages) infiltration as well as the presence of mast cells (intact or degranulated) were determined in the different areas of the skin and in the granuloma. The number of fibroblasts was also monitored. Data are reported as number of cells per $100 \times 100$ $\mu m^2$ of tissue area.

## Biochemical determinations

*Detection of chemokine levels by ELISA* Samples were placed in lysing buffer (1% P-40 Nonidet, 500 mM NaCl, 50 mM HEPES, 20 μg/ml leupeptin) (Standiford *et al.*, 1995) at an approximate ratio of 10 mg $ml^{-1}$ and homogenized using a T25 IKA Labortechnik homogenizer (Staufen, Munich, Germany). Chemokine levels were measured in tissue supernatants using commercially available ELISA kits for mouse MIP-1α, MIP-2, KC and RANTES (R&D

Systems, Abingdon, Oxon, U.K.) and MCP-1 (Biosource International, Camarillo, CA, U.S.A.).

*Enzymatic activities* Myeloperoxidase (MPO) and N-acetyl-β-D-glucosaminidase (NAG) activity in tissue supernatants were determined as an indirect measurement of neutrophil and monocyte influx (Bailey *et al.*, 1982; Mullane *et al.*, 1985).

The MPO reaction was performed in 200 μl total volume using 2 mM 3,3',5,5'-tetramethyl-benzidine (Sigma-Aldrich) in 50 mM acetate buffer (pH 6) as a substrate, and hydrogen peroxide (20 μl of a solution 30% v $v^{-1}$). After 30 min at room temperature, absorbance was read at 620 nm wavelength and interpolated on a standard curve constructed with $0-2000$ mu $l^{-1}$ human neutrophil MPO (Calbiochem, Beeston, Nottingham, U.K.). Data are expressed as mu mg $protein^{-1}$.

The NAG reaction was performed in 250 μl total volume containing unknown sample and the substrate *p*-nitrophenyl-N-acetyl-β-D-glucosaminide (2.5 mM in 50 mM citrate buffer, pH, 4.5) (Sigma-Aldrich). After 45 min incubation at 37°C, the reaction was initiated by adding 100 μl of glycine buffer (0.2 M, pH 10.4; BDH Laboratory Supplies). Readings at 405 nm wavelength were interpolated on a standard curve constructed with *p*-nitrophenol ($0-500$ nmol $ml^{-1}$) (Sigma-Aldrich). Data are reported as nmol of products formed mg $protein^{-1}$.

Protein concentration in the homogenized tissue samples was determined by the Bradford assay (Biorad Protein Assay, BioRad Laboratories GmbH, Munchen, Germany).

## TaqMan® reverse-transcriptase-polymerase chain reaction (RT–PCR) analysis

TaqMan real-time RT–PCR assay allows reliable, reproducible and accurate measurement of mRNA expression following activation of a given gene (Gibson *et al.*, 1996; Heid *et al.*, 1996; Hirayama *et al.*, 1998; Lie & Petropoulos, 1998; Orlando *et al.*, 1998). Here, this technique was applied to monitor chemokine and chemokine receptor expression. Total RNA was extracted from pooled samples of skin or granuloma tissue ($n = 5-10$), following homogenization with a T25IKA Labortechnik homogenizer pre-sterilized in a bath of Trigene® solution (2%) overnight. To avoid contamination, the homogenizer was cleaned with ethanol, Trigene® solution and sterile water between each tissue sample. The RNA yield and purity was determined by the $A_{260}/A_{280}$ ratio and the integrity of total RNA extracted was confirmed by the presence of 28S and 18S bands following electrophoresis on a 1% agarose gel. RNA was further purified by selective precipitation, using RNeasy® mini-spin columns (QIAGEN, Crawley, West Sussex, U.K.) and stored at $-80°C$ until use. cDNA was synthesized using Superscript II kit (GIBCO-BRL, Life Technologies Ltd, Paisley, Scotland, U.K.), with 2 μg of total RNA being converted into cDNA by addition of 1 μl of Superscript II reverse transcriptase (RTEnzyme®, $10,000-50,000$ units $ml^{-1}$) (GIBCO-BRL). Negative controls were obtained by reverse transcriptase omission. A standard curve to calculate relative amounts of transcript in unknown samples was constructed using cDNA generated from the lymph nodes of oxazolone-treated mice.

TaqMan® fluorogenic probes used were -FAM (6-carboxi-fluorescein; emission 1538 nm) or -JOE (6-carboxy-4,5-

dichloro-2,7-dimethoxyfluorescein; emission 1546 nm) reporter and TAMRA (6-carboxytetramethylrodamine; emission 1582 nm) quencher dyes (Applied Biosystems, Foster City, CA, U.S.A.). Primers and probes were designed in accordance to the 'guidelines for designing TaqMan® fluorogenic probes for 5′ nuclease assay' (provided by Perkin Elmer Applied Biosystems). Primers were obtained from Genosys (Sigma-Genosys Ltd, Pampisford, Cambridgeshire, U.K.) and optimized using a standard cDNA template. Table 1 summarizes the sequences of the probes and primers used. TaqMan® reactions were set up as indicated by the manufacturers and amplified using the ABI PRISM 7700 Sequence Detection System. cDNA prepared from granuloma samples was diluted 1/10 and tested in duplicate or triplicate in the TaqMan® RT–PCR assay. Primers and probes were also designed for MIP-1α and CCR1 and tested without success.

For each well a mixture of forward and reverse primers, probes and TaqMan® Master Mix (AmpliTaq Gold DNA Polymerase, AmpErase UNG, dNTPs with dUTP) (GIBCO BRL) was added (see Table 2 for the optimal ratios). Cycling conditions for the TaqMan® PCR reactions were as follows: 2 min at 50°C, 10 min denaturation at 95°C, 15 s annealing at 95°C and 1 min extension at 60°C. For data handling, a standard curve was constructed from a scatter plot of log dilution factor *vs* the corresponding threshold cycle ($C_T$) and used to calculate the relative abundance of each target gene in each sample. 18S $C_T$ values were used to correct for the amount of cDNA in each sample and give a normalized relative amount for each sample.

### Treatment with neutralizing antisera

The same antisera used for immunocytochemistry of MIP-1α and MCP-1 were also used for assessing the function *in vivo* that either chemokine might have. Both rabbit sera have been validated for the respective chemokine *in vitro* and *in vivo* assays (Chensue *et al.*, 1996; DiPietro *et al.*, 1998; Kunkel *et al.*, 1996; Standiford *et al.*, 1995).

The anti-MIP-1α rabbit serum, or non-immune rabbit serum (Sigma-Aldrich), were given i.p. at the dose of 0.5 ml per mouse (Di Pietro *et al.*, 1998) per injection on days −1, +1 and +4, with CO/CFA being injected into the air-pouch at day 0. Animals were sacrificed at days 7 or 21, since these times corresponded approximately to the peaks of the MIP-1α and MCP-1 protein levels.

The anti-MCP-1 rabbit serum has been used shown to be active in a murine model of lethal endotoxemia (Zisman *et al.*, 1997). Its activity has also been shown in a model of granuloma formation in which repeated injections decreased the size of the granuloma by about the 30% (Chensue *et al.*, 1996). Since the peak of MCP-1 occurred at day 21, the antibody, or non-immune rabbit serum, were given i.p. at the dose of 0.5 ml per mouse on days 10 and 14, and animals sacrificed on day 21.

In both cases a series of biochemical determinations in the granuloma samples was made.

### Statistics

Differences among groups were analysed using ANOVA plus Bonferroni test taking a *P* value <0.05 as significant. Non-

**Table 1** Sequence for probes and primers of the genes of interest. All sequences follow 5′-3′ direction

| Gene of interest | Probe | Forward primer | Reverse primer |
| --- | --- | --- | --- |
| CXCR2 | CAGAAGCACCGGGCCATGCG | CACCCTCTTTAAGGCCCACAT | ACAAGGACGACGACAGCGAAGATG |
| CCR2 | ACAGAGACTCTTGGAATGACACACTGCTGC | AGTAACTGTGTGATTGACAAGCACTTAGA | CAACAAAGGCATAAATGACAGGAT |
| CCR5 | TACCTGCTCAACCTGGCCATCTCTGA | CATCGATTATGGTATGTCAGCACC | CAGAATGGTAGTGTGAGCAGGAA |
| KC | CGCTGTCAGTGCCTGCAGACCATG | GGCGCCTATCGCCAATG | CTGGATGTTTCTTGAGGTGAATCC |
| MIP-2 | TGACGCCCCCAGGACCCCA | TGACTTCAAGAACATCCAGAGCTT | CTTGAGAGTGGCTATGACTTCTGTCT |
| LIX | CGCCGCTGGCATTTCTGTTGCT | TTCCAGCTCGCCATTCATG | AGCTCCGTTGCGGCTATG |
| MCP-1 | TTAACGCCCCACTCACCTGCTGCTACT | GTTGGCTCAGCCAGATGCA | AGCCTACTCATTGGGATCATCTTG |
| MCP-3 | CCTGCTGCTCATAGCCGCTGCTTT | GGATCTCTGCCACGCTTCTG | GGCCCACACTTGGATGCT |
| MIP-1β | CTCTGACCCTCCCACTTCCTGCTGTTT | AGGGTTCTCAGCACCAATGG | GCTGCGGGAGGTGTAAGA |
| RANTES | CGCCAAGTGTGTGCCAACCCA | GTCGTGTTTGTCACTCGAAGGA | TTGATGTATTCTTGAACCCACTTCTT |

The sequences of probes and primers shown were designed as described in the Methods section, and used for TaqMan® analysis.

**Table 2** Concentration and optimal ratio of genes of interest

| Gene of interest | PROBE (pmol $\mu l^{-1}$) | Forward primer (pmol $\mu l^{-1}$) | Reverse primer (pmol $\mu l^{-1}$) | Optimal ratio (nM) |
|---|---|---|---|---|
| CXCR2 | 5 | 4.7 | 10.8 | 300:300 |
| CCR2 | 5 | 4.7 | 9.3 | 300:300 |
| CCR5 | 5 | 12.8 | 11.4 | 300:300 |
| KC | 5 | 10 | 10 | 300:300 |
| MIP-2 | 5 | 10 | 10 | 900:900 |
| LIX | 5 | 100 | 100 | 900:300 |
| MCP-1 | 5 | 10.3 | 13.2 | 300:300 |
| MPC-3 | 5 | 12.9 | 9.2 | 300:300 |
| MIP-1β | 5 | 11.4 | 11.1 | 50:50 |
| RANTES | 5 | 6.4 | 12.6 | 50:50 |

Shown are the concentrations of probes and primers and the optimal ratios, in relation to $C_T$ values, as used for TaqMan® analysis.

parametric Kruskal-Wallis analysis was used for TaqMan® data. Instat™ software was run on an Apple Macintosh G3.

## Results

### CO/CFA, but not IFA, injection provokes granuloma formation

CO/CFA injection produced formation of granulomatous tissue already detectable at day 3. The tissue wet weight increased in a time dependent manner until day 7, decreasing thereafter (Figure 1). In contrast, IFA injection did not produce formation of granuloma, and the weight of the tissue did not significantly change throughout the entire time course.

These differences were confirmed by histology. IFA caused only a large increase in the thickness of the adipose tissue (Figure 2A illustrates the morphology at day 14) when compared to the skin of control mice (Figure 2B). CO/CFA produced a series of time-dependent changes illustrated from Figure 2C to G. On day 3, the presence of the granulomatous tissue under the skeletal muscle layer was detected (Figure 2C). The thickness of the granuloma doubled by day 7 (Figure 2D), with a similar appearance at day 14 (Figure 2E). A contraction of the granulomatous tissue, replaced by fibrotic tissue mainly formed by collagen, was observed on day 21 (Figure 2F). A similar pattern was observed at day 28 (Figure 2G).

The majority of the cells in the granuloma were PMN and MNC. Fibroblasts could also be seen, whereas mast cells were predominantly found in the skin layers. The localization and the numbers of the different cells varied throughout the time-course (Figure 3). An increase in MNC was observed by day 7 in the granulomatous layer, decreasing by days 14 to 21, thereafter increasing again at day 28 (Figure 3D). The same profile was detected in the adipose tissue (Figure 3B), but not in the dermis and in the skeletal muscle layer, where MNC infiltration decreased from day 7 onwards (Figure 3A,C). Similar changes were detected in PMN influx throughout the tissue layers: following a peak at day 7 and a time-dependent reduction by day 21, a second phase of influx into the granulomatous and adipose tissue layers was apparent at day 28 (Figure 3). However, the changes in the granuloma were more pronounced with PMN and
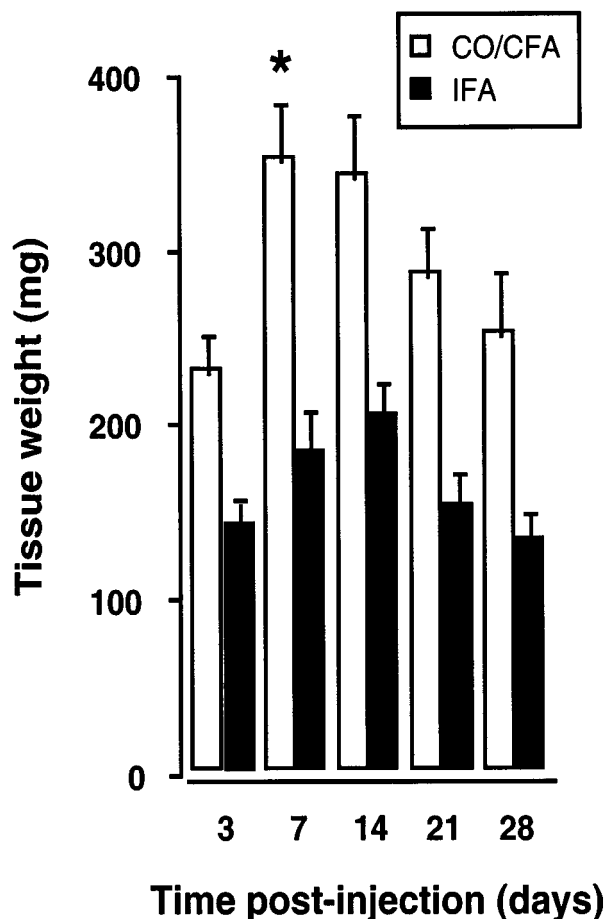


**Figure 1** Time-course of granuloma weight after CO/CFA or IFA injection into murine air-pouches. Change in the weight of inflamed tissue after local injection of 0.5 ml IFA or CO/CFA mixture. Note that granuloma formation occurs only after CO/CFA injection (see Figure 2). Data are mean±s.e.mean of eight mice per group. *$P < 0.05$ *vs* day-3 group.

MNC counts, 5–10-fold higher than those counted in the skin layers. An approximate 2–3-fold increase in mast cell numbers was measured in all tissue layers by days 7 and 14 post-inflammation, 50% of which were degranulated (data not shown). Detection of cells became difficult by day 21 in the skeletal muscle tissue probably because of

the replacement of this tissue with the fibrotic fibres (Colville-Nash *et al.*, 1995). Fibroblast cell numbers increased in the granulomatous tissue from day 14 onward with highest values at day 28 (Figure 3).
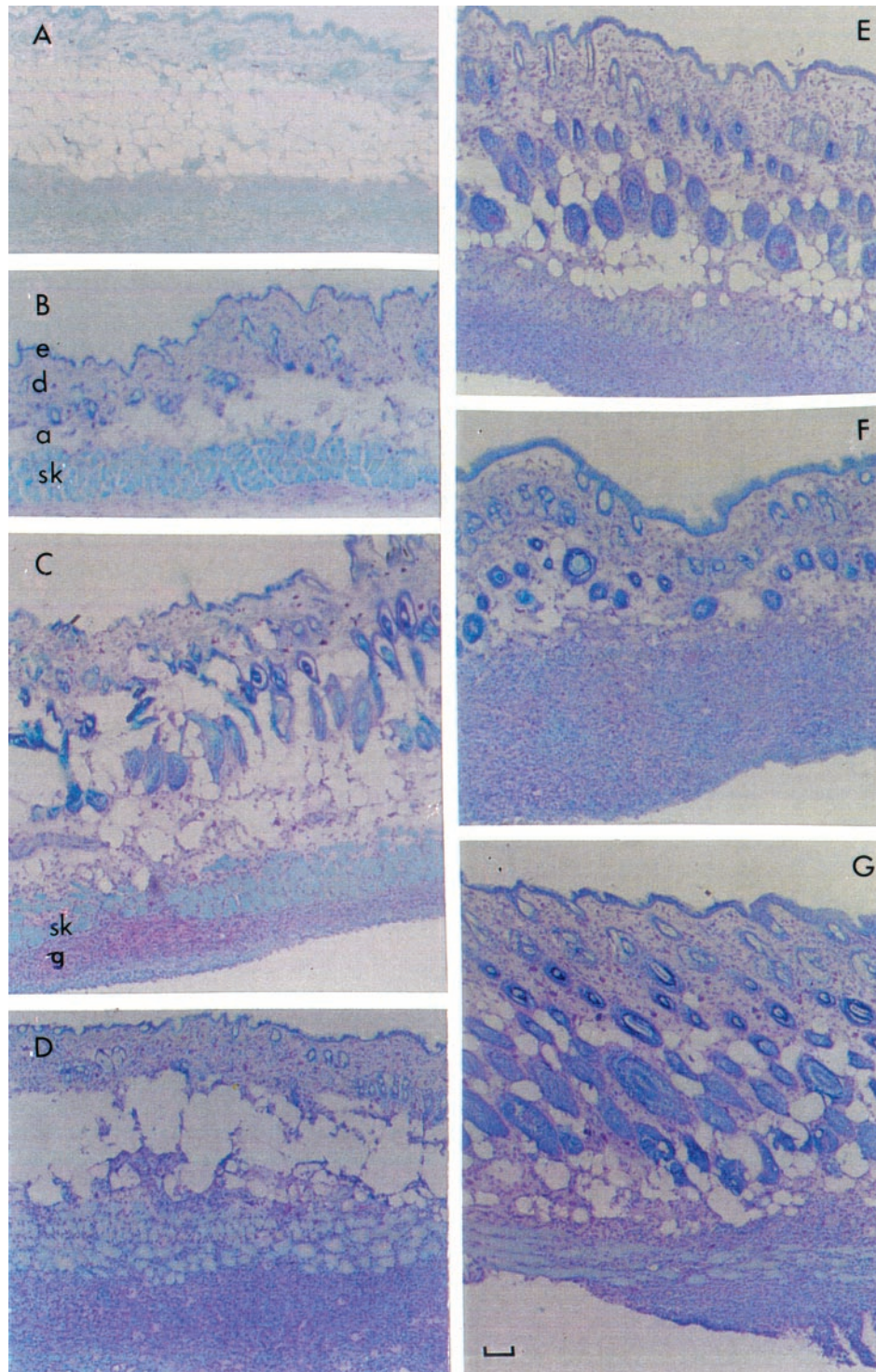


**Figure 2** Histological features of inflamed tissues after CO/CFA or IFA injection into murine air-pouches. (A): May-Grumwald-Giemsa staining of sections (1.5 μm) obtained from historesin embedded tissues, showing morphology of the air-pouch 14 days after IFA injection. (B) to (G): toluidine blue staining on cryostat sections (10 μm). In (B) skin morphology of an untreated mouse, with the epidermal layer (e), the dermis (d), the subcutaneous tissue (or hypodermis) consisting mainly of adipose tissue (a), represented by white globular cells and skeletal muscle cells (sk), stained in light blue. From (C) to (G) the response to CO/CFA injection. On day 3 (C), granulomatous tissue (g) can be localized under the skeletal muscle layer (sk), with increased thickness on day 7 (D) and day 14 (E). Proliferation of fibrotic tissue (not shown with this staining) and reduction of granuloma tissue occurred between day 21 (F) and day 28 (G). Pictures are representative of 10 distinct analyses. Bar, 150 μm.
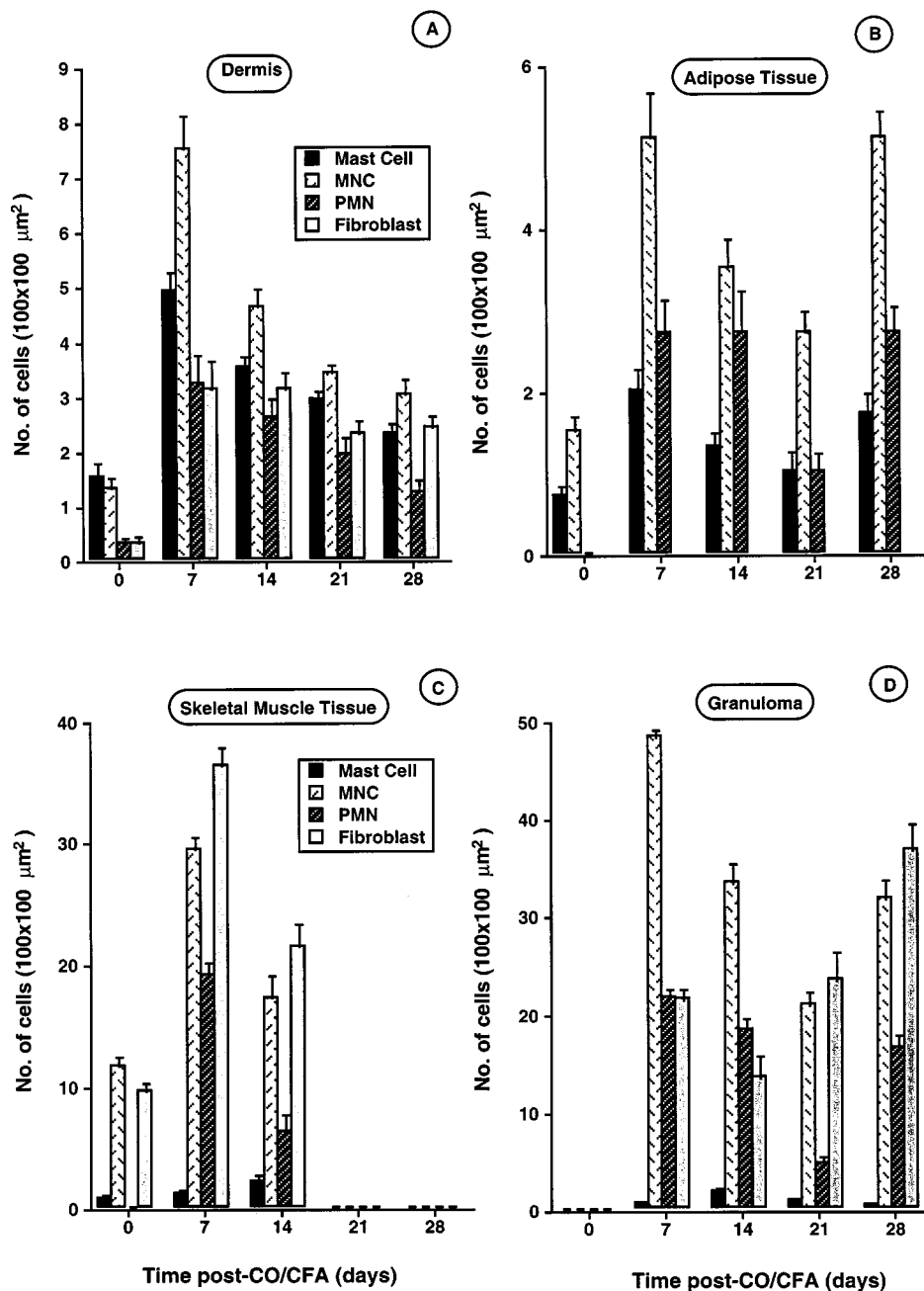
**Figure 3** Semi-quantitative analysis of cell population in the different skin layers and granulomatous tissue during CO/CFA induced inflammation. Tissues (skin or granuloma) were embedded in historesin, stained and analysed as described in Methods. Analysis could distinguish between mast cells, MNC, PMN and fibroblasts present in the dermis (A), adipose tissue (B), skeletal muscle tissue (C) and granulomatous tissue (D). Values represent mean $\pm$ s.e.mean of cell number counted in three different regions of $100 \times 100$ $\mu m^2$ area, five distinct serial sections (1.5 $\mu m$) of four different mice.

*Enzymatic activities in the granuloma*

MPO activity increased rapidly ($\sim$30 mu mg protein$^{-1}$ per day) up to day 7 post-CO/CFA injection (Figure 4A). In line with histological quantification, lower MPO values were measured at days 14 and 21, with a subsequent increase at day 28 (Figure 4A). High MPO values clearly corresponded to PMN infiltration, as seen in Figure 4C. NAG activity followed a different profile, with values above skin controls from day 7, and a time-dependent increase up to the fourth week of

inflammation (Figure 4B). The majority of MNC had migrated by day 28 as determined by morphology (Figure 4D). However, PMN were also present at this time-point (data not shown).

*Chemokines and chemokine receptors in the granuloma*

The mRNA expression of CXCR2 showed a single peak maximal at day 3. Relatively high amounts of this mRNA were also detected at day 7, after which values decreased rapidly towards control (Figure 5A). Of the three potential CXCR2
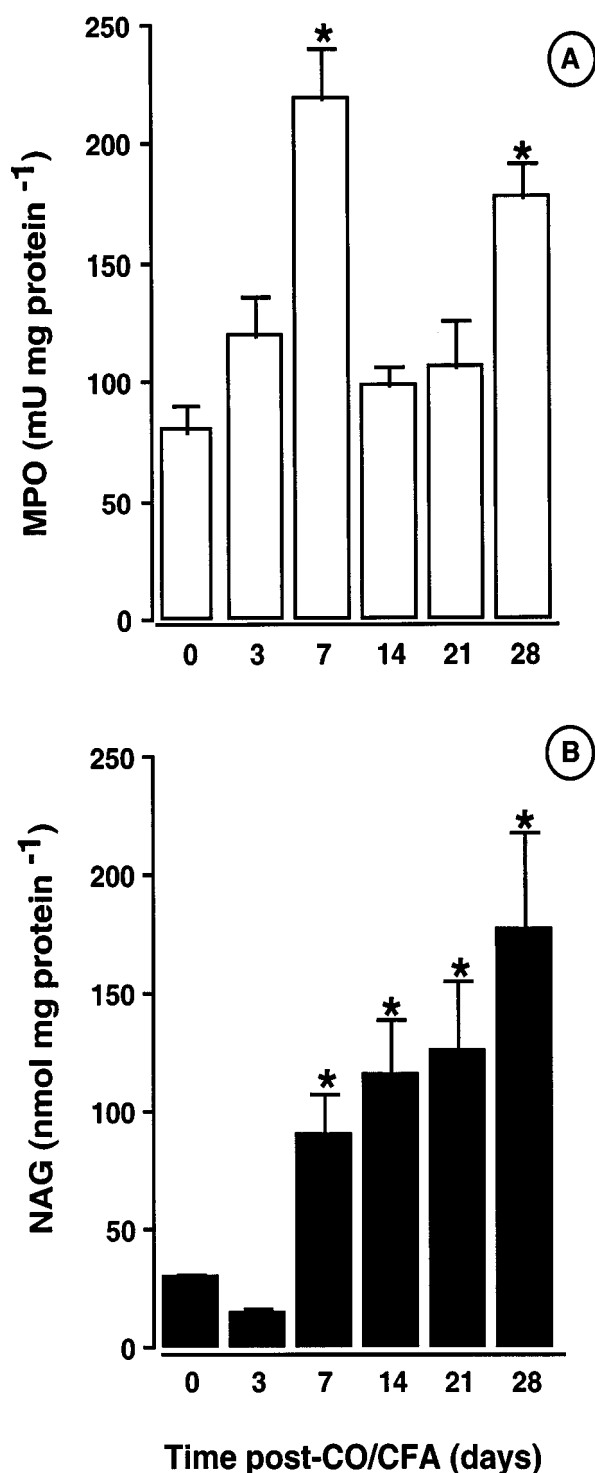
**Figure 4** Enzymatic activities and infiltrating cells associated with granulomatous tissue. (A) Time-course of MPO activity and (B) NAG activity as measured in the granulomatous tissue. May-Grumwald-Giemsa staining of historesin sections (1.5 $\mu$m) showing (C) an intense PMN influx on day 7 (arrows) and (D) the presence of MNC (indicated by open arrows) on day 28. Values are mean$\pm$ s.e.mean of $>10$ mice per group, whereas pictures are representative of three different mice *$P<0.05$ *vs* control (non inflamed) group. Bar, 20 $\mu$m.

ligands tested, KC (CXCL1) and MIP-2, but not LIX (CXCL5), mRNA were detected and found to be maximal at day 3, in correspondence to the CXCR2 mRNA (Figure 5B).

The profile of CCR2 and CCR5 mRNA expression was less clear, and changes were less pronounced (Figure 5C,E). The mRNA for some putative ligands for these receptors was also increased, though with some differences. Figure 5D shows MCP-1 (CCL2) mRNA being high at days 3 and 28, whereas MCP-3 (CCL7) mRNA highest values are measured at days 14 and 28. MIP-1$\beta$ (CCL4) and RANTES (CCL5) follow a similar pattern of expression, with MIP-1ß mRNA being clearly highly expressed during the first week of inflammation (Figure 5F).

Chemokine protein expression within the granulomatous tissue paralleled the detection of mRNA. KC (CXCL1) and MIP-2 protein were clearly elevated within the first week of inflammation as detected by ELISA (Figure 6A). MIP-1α (CCL3) was maximally expressed at day 3 (Figure 6B), whereas MCP-1 (CCL2) levels increased in a time-dependent fashion, with values above control skin samples at day 21 (Figure 6C). RANTES (CCL5) protein expression increased gradually in a time-dependent fashion with maximal values at day 28 (Figure 6D).

### Immunohistochemistry for MIP-1α and MCP-1

The cell source of two chemokines that were expressed at different stages of this experimental inflammatory reaction was then investigated. In the granulomatous tissue of samples collected at day 7 post CO/CFA injection, MIP-1α immunoreactivity was detected in fibroblasts (Figure 7A) and MNC (Figure 7B). After the first week of inflammation, the number of positive cells decreased in accordance with the data obtained by ELISA (data not shown). MCP-1 localization was studied in correspondence of the peak of protein expression, i.e. at day 21 (Figure 6C). A part from some scattered MNC and fibroblasts (Figure 7E), MCP-1 immuno-reactivity was predominantly associated with mast cells (Figure 7D,F). The identity of this cell type was also confirmed by counter-staining with toluidine blue (data not shown). No staining was visualized in sections stained with pre-adsorbed antibody (Figure 7C).

### Effect of neutralizing antisera to MIP-1α and MCP-1

Treatment of mice with the anti-MIP-1α serum did not significantly modified the inflammatory response as measured at day 7, with the exception of a reduction in MIP-1α contents (Table 3). In contrast, animals treated with the anti-MIP-1α serum displayed higher values for inflammatory parameters at day 21, namely for MPO activity, NAG activity and MCP-1 contents (Table 3).

The anti-MCP-1 serum was tested only at day 21, since this time-point corresponded to the peak of endogenous MCP-1 expression (see Figure 6c). Table 4 shows the data obtained, with a significant decrease ($\sim40\%$) in NAG activity and a reduction in the content of RANTES. This was associated with a significant increase in MPO values (Table 4).

## Discussion

The granulomatous air-pouch has been previously employed to study the profile of expression of pro-inflammatory and

anti-inflammatory cytokines, mainly using an immunohisto-chemistry strategy (Appleton *et al.*, 1993). The interest in this model stems from the morphological analogies between the experimental granuloma and the pannus observed in the joints of patients affected by rheumatoid arthritis, for instance presence of resident macrophages and fibroblasts (Kimura *et al.*, 1985; 1986; Kasama *et al.*, 1995). Injection of CO/CFA initiates a complex inflammatory reaction. Based on distinct patterns of expression, and on the appearance of PMN and MNC into the granuloma, the existence of an
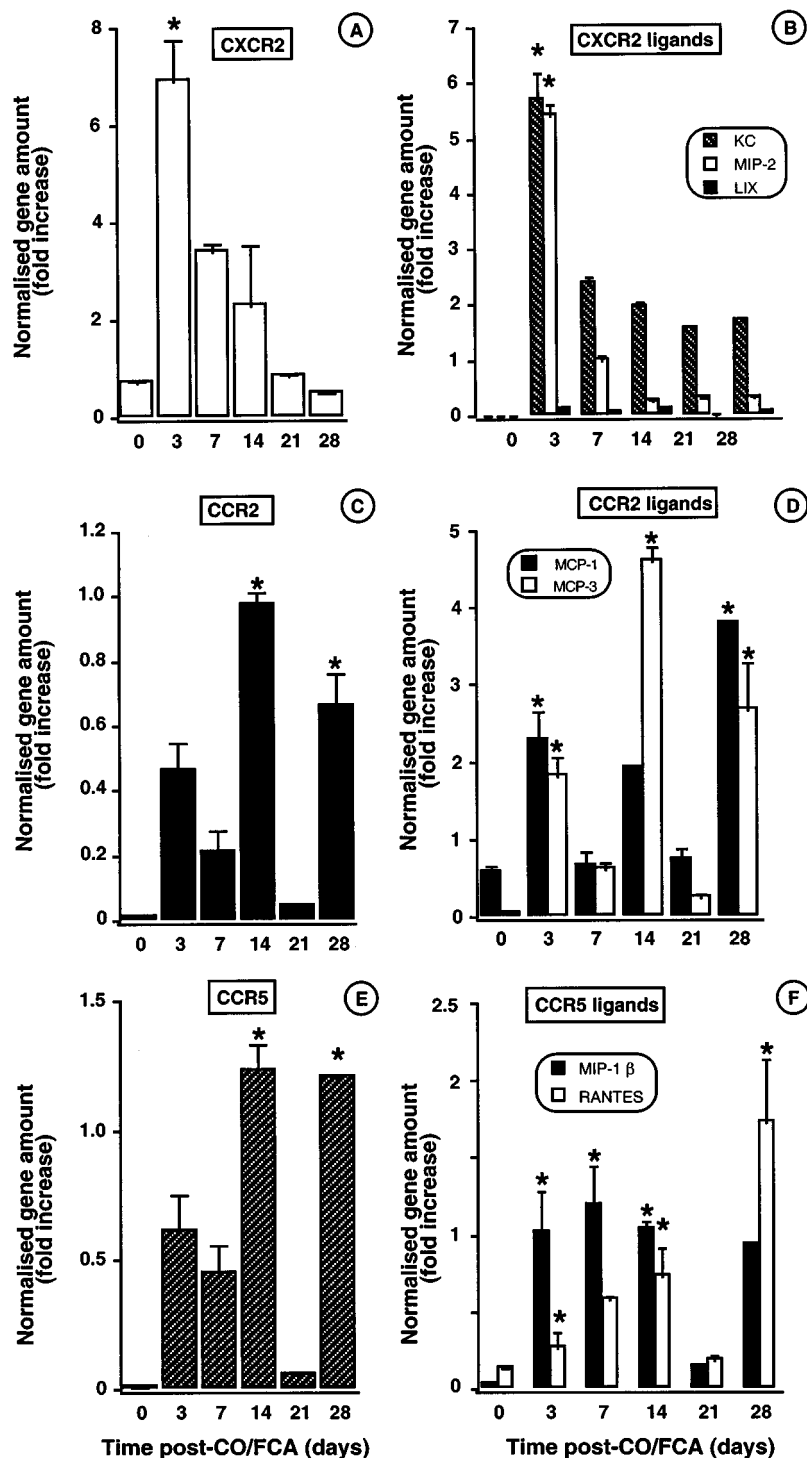


**Figure 5** Time-course of mRNA chemokine and chemokine receptor expression during CO/CFA inflammation as determined by TaqMan® RT – PCR analysis. Quantification of the following mRNA was made in granulomatous tissue samples. (A) CXCR2 and (B) CXCR2 ligands; KC, MIP-2 and LIX. (C) CCR2 and (D) CCR2 ligands; MCP-1 and MCP-3; (E) CCR5 and (F) CCR5 ligands; MIP-1β and RANTES. Values are fold increase of gene amount normalised against the 18S gene and expressed as mean ± s.e.mean of >10 mice per group. *$P < 0.05$ *vs* control (non inflamed) skin.
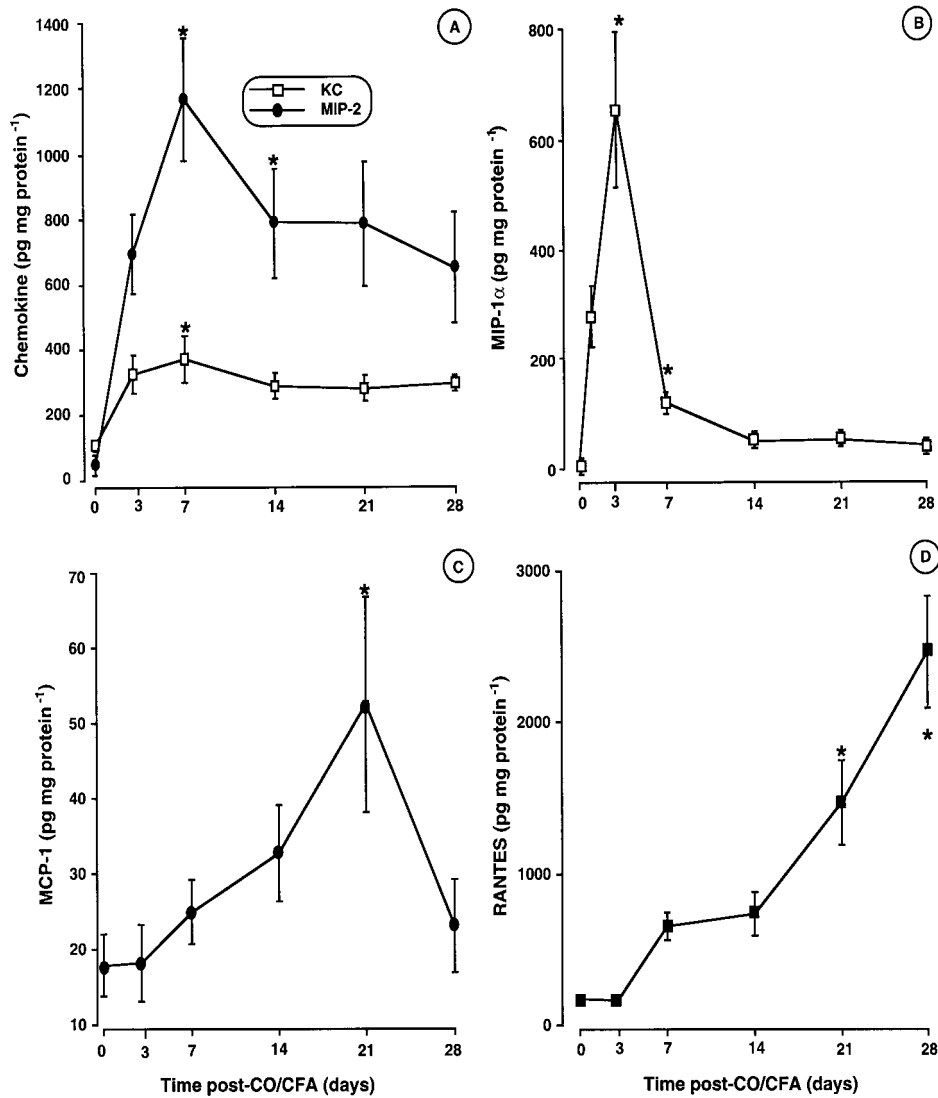
**Figure 6** Chemokine protein levels during CO/CFA inflammation. (A) Granuloma content of KC and MIP-2, (B) MIP-1α, (C) MCP-1 and (D) RANTES protein levels. Values are mean±s.e.mean of >10 mice per time-point, *$P<0.05$ *vs* control (non inflamed) skin.

**Table 3**    Effect of the anti-MIP-1α polyclonal serum on selected markers of the granulomatous air-pouch inflammation

| Marker of inflammation (units) | Anti-MIP-1α serum | Non-immune rabbit serum |
|---|---|---|
| **Day 7** | | |
| Granuloma wet weight (mg) | 345±41 (8) | 488±54 (4) |
| MPO (mU mg protein$^{-1}$) | 189±20 (8) | 224±16 (4) |
| NAG (mmol mg protein$^{-1}$) | 77±8 (8) | 62±22 (4) |
| MIP-1α (pg mg protein$^{-1}$) | 664±60 (8)* | 1263±84 (4) |
| **Day 21** | | |
| Granuloma wet weight (mg) | 273±84 (6) | 264±32 (4) |
| MPO (mU mg protein$^{-1}$) | 275±21 (6)* | 139±22 (4) |
| NAG (nmol mg protein$^{-1}$) | 87±6 (6)* | 54±11 (4) |
| MCP-1 (pg mg protein$^{-1}$) | 191±31 (6)* | 123±21 (4) |
| RANTES (pg mg protein$^{-1}$) | 4286±745 (6) | 5187±316 (5) |

Animals were treated with the mixture of CO/CFA at day 0, and with non-immune rabbit serum or with the anti-MIP-1α antiserum at days −1, 1 and 4 (500 μl i.p. each time). Tissues were collected either at day 7 or day 21, and the different markers of inflammation determined as described in Methods. Values shown are the mean value±s.e.mean of (*n*) mice per group. *$P<0.05$ *vs* corresponding value in the non-immune serum group.
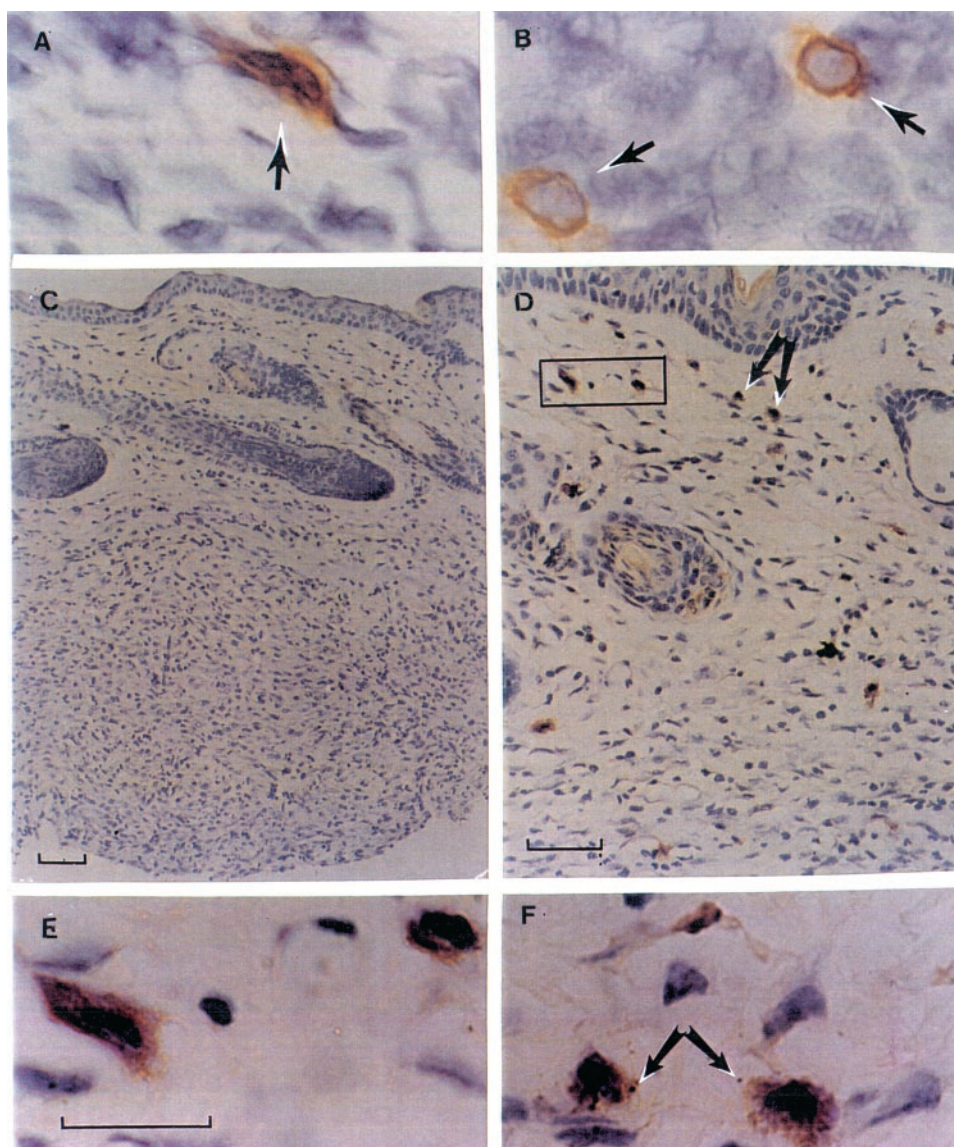
**Figure 7** Localization of MIP-1α and MCP-1 in the granulomatous tissue. Cryostat sections (10 $\mu$m) showing (A) MIP-1α staining in fibroblasts (arrow) and (B) in MNC (likely to be macrophages, arrows). (C) Negative control of pre-absorbed MCP-1 polyclonal antibody on paraffin embedded sections (3 $\mu$m). (D) Immunoreactivity for MCP-1 in fibroblasts and mast cells localized mainly in dermis and some scattered mast cells in the granuloma layer. (E) High magnification of fibroblasts and MNC cells MCP-1 positive detected in dermis in the rectangular field in (D). (F) High magnification of mast cells MCP-1 positive observed in dermis layer indicated by the arrowhead in (D). Bar, 20 $\mu$m for panels A, B, E and F; bar, 50 $\mu$m panel D and 100 $\mu$m panel C.

**Table 4** Effect of the anti-MCP-1 polyclonal serum on selected markers of the granulomatous air-pouch inflammation

| Marker of inflammation (units) | Anti-MCP-1 serum | Non-immune rabbit serum |
|---|---|---|
| Granuloma wet weight (mg) | $318 \pm 53$ (8) | $287 \pm 69$ (5) |
| MPO (mU mg protein$^{-1}$) | $203 \pm 18$ (8)* | $101 \pm 14$ (5) |
| NAG (nmol mg protein$^{-1}$) | $158 \pm 19$ (8)* | $276 \pm 21$ (5) |
| MCP-1 (pg mg protein$^{-1}$) | $101 \pm 25$ (8) | $83 \pm 25$ (5) |
| RANTES (pg mg protein$^{-1}$) | $1722 \pm 189$ (8)* | $2814 \pm 398$ (5) |

Animals were treated with the mixture of CO/CFA at day 0, and with non-immune rabbit serum or with the anti-MCP-1 antiserum at days 10 and 14 (0.5 ml i.p. each time). Tissues were collected either at day 7 or day 21, and the different markers of inflammation determined as described in Methods. Values shown are the mean value $\pm$ s.e.mean of (*n*) mice per group. * $P < 0.05$ *vs* corresponding value in the non-immune serum group.

acute phase (maximal within the first week) and of repair phase (from day 21 onwards) has been proposed (Appleton et al., 1993).

Initially, we validated the model. We could demonstrate the presence of layers of granulomatous tissue from day 3, with a time-dependent progressive thickening. Day 7 corresponded to the time-point of maximal PMN infiltration and the presence of characteristic signs of an intense inflammatory reaction, including mast cell degranulation. It has been demonstrated that this stage presents a high incidence of neo-vessel formation (angiogenesis) (Colville-Nash et al., 1995). These events occur also at the skin level, with leukocyte infiltration into the derma and hypoderma. However, quantitatively, the major portion ($>80\%$) of blood-borne cells migrated into the granuloma.

The existence of a PMN influx within the first week was confirmed by measurement of MPO activity. Assessment of this enzyme has often been used to determine tissue infiltration by PMN (Mullane et al., 1985). MPO measurement coupled to histology and the expression of PMN selective chemokines (see below) suggest that the first week of this inflammatory reaction was predominantly characterized by PMN accumulation. The striking expression of CXCR2 in the granuloma at days 3 and 7 confirms this suggestion, since PMN express high levels of this receptor (Murphy et al., 1996).

CXCR2 mRNA expression was paralleled by expression of its ligands both at the mRNA and protein level. In particular, MIP-2 and KC were strongly expressed within the first week of inflammation, whereas the recently discovered CXC chemokine LIX was not. Differences in time expression of these three chemokines have been reported during experimental endotoxemia (Rovai et al., 1998), but are unlikely to explain the lack of detection of LIX mRNA in this model. A few days of delay were observed in terms of peak of mRNA and protein expression for MIP-2 and KC: this is not surprising and may indicate the existence of mechanism(s) for controlling mRNA translation. We have observed a similar feature for granuloma expression of the anti-inflammatory protein annexin-1 (unpublished data). A human analogue of the CXC murine chemokine KC (likely to be gro-α; Zlotnik & Yoshie, 2000) is detected in synovial fluids of patients affected by rheumatoid arthritis, with synovial fibroblasts being the major cell source (Koch et al., 1995): it is possible that KC-related chemokines play a functional role in attracting human PMN into the injured joints.

A difference in the time course of expression between the two CC chemokines MIP-1α and MCP-1 was observed in this model of chronic inflammation. MIP-1 α seems to play an important role in human rheumatoid arthritis (Koch et al., 1995), and its mRNA is abundantly expressed in the joints during mouse collagen-induced arthritis (Kasama et al., 1995; Kunkel et al., 1996). This CC chemokine acts as a chemoattractant on both PMN and MNC (DiPietro et al., 1998; Ajuebor et al., 1999), however the profile of expression in this model indicates a major effect upon the PMN. In addition, MIP-1α activates mast cells (Alam et al., 1992) and therefore may contribute to the degranulation of this cell type observed from day 3 post-CO/CFA injection. In view of the pivotal role that mast cell-derived products play in the recruitment of PMN (Granger & Kubes, 1994), it is tempting to propose a model in which MIP-1α plays central

role in the first week of inflammation (the so-called 'acute phase' of Appleton et al., 1993). Other chemokines such as KC may also have a prominent role in producing mast cell activation (Harris et al., 1996). The neutralization experiments however indicate that if MIP-1α plays a pro-inflammatory role within day 7, it is clear that its role can be taken over by other mediators or chemokines. The set of functional data indicates, rather, that early MIP-1α expression possesses an anti-inflammatory role on the progression of the granulomatous inflammation. It is of interest that MIP-1α expression has been associated with murine wound repair (DiPietro et al., 1998).

MCP-1 expression was clearly associated with this latter phase characterized by deposition of collagen fibres, fibroblast proliferation and fibrosis (Appleton et al., 1993; Colville-Nash et al., 1995). The existence of mechanism(s) regulating mRNA translation, or the potential need for accessory factors, are likely to be involved for MCP-1 since a modest increase in MCP-1 mRNA was detected at day 3, but the protein was not detectable by ELISA. The second peak of MCP-1 mRNA was linked to the presence of MCP-1 protein, from day 14 onward. RANTES mRNA and protein followed a similar profile of expression.

At variance from the hypothesis of Appleton et al. (1993), who proposed the existence of a process of resolution from day 14 onward, in our hands many parameters of inflammation were still elevated or present even at day 28. In fact, whereas low values were measured at day 21 for several parameters, including PMN and MPO activity, chemokine and chemokine receptor mRNA, clear signs of an active inflammatory response were measured at day 28: mast cell degranulation and PMN infiltration were clearly seen in the granuloma. This was also associated to high MPO activity, besides the expected high value for NAG activity. It is now clear that monocytes also contain MPO positive granules, and therefore can contribute to tissue appearance of this enzymatic activity (Dallegri & Ottonello, 1997; Korthuis et al., 1994; Marquez & Dunford, 1997). Therefore, in contrast to previous publications on this model of granuloma, we would propose the presence of a process of fibrosis characterizing the second phase of inflammation from day 14 onwards. Importantly, MCP-1 has been shown to be a potent pro-fibrotic chemokine (Hogaboam et al., 1999), whereas RANTES does not share this activity (Lloyd et al., 1997). Together with a published study (Appleton et al., 1993), we propose a fibrotic alteration of the granuloma driven initially by transforming growth factor-$\beta$ (that peaks at day 14), and subsequently by MCP-1. In this scenario, RANTES may contribute in an as yet unknown manner to the chronicization of the inflammatory reaction, as recently shown in an experimental model of inflammatory bowel disease (Ajuebor et al., 2001).

The experiment of neutralization supports, to our opinion, this hypothesis. The anti-MCP-1 antiserum reduced NAG activity and RANTES values, and elevated MPO activity, as measured at day 21. It may be proposed, then, that MCP-1 and possibly RANTES recruit monocyte/macrophages at this time-point. Importantly, NAG is expressed at higher levels by differentiated macrophages (de Moulder et al., 1983). The higher MPO values observed in the anti-MCP-1 group may indicate a lower degree of removal of migrated PMN caused by the lower number of macrophages.

Finally, the availability of two anti-sera validated for detection of MIP-1α and MCP-1 in tissues allowed us to monitor the cellular localization of these chemokines at the peak of their expression. Monocyte/macrophages and fibro-blasts were positive for MIP-1α in the 7 day-granuloma. This finding is in agreement with other experimental models of inflammation (Chensue *et al.*, 1996; di Pietro *et al.*, 1998; Kunkel *et al.*, 1989; Standiford *et al.*, 1993). MCP-1 was predominantly expressed by mast cells located in the granuloma as well as in the surrounding skin layers. We believe this is an important observation, and linked to other studies (Tailor *et al.*, 1999) it suggests mast cells as a major source of CXC and CC chemokines in inflammation. With respect to this specific chemokine, we have recently found that mouse peritoneal mast cells are the major producers of MCP-1 during acute peritonitis (Ajuebor *et al.*, 1999). It therefore seems that mast cells have the capacity to synthesize several inflammatory mediators, including chemokines, and therefore have a prominent role in many forms of inflammation. Importantly, cell responsiveness to MCP-1 is altered during experimental chronic inflammation (Johnston *et al.*, 1999). If this phenomenon also occurs in our model of granulomatous air-pouch, then we propose that mast cell derived MCP-1 may be responsible for the delayed (>21 days) neutrophil recruitment.

## References

AJUEBOR, M.N., DAS, A.M., VIRÁG, L., FLOWER, R.J., SZABÓ, C. & PERRETTI, M. (1999). Role of resident peritoneal macrophages and mast cells in chemokine production and neutrohil migration in acute inflammation: evidence for an inhibitory loop involving endogenous IL-10. *J. Immunol.*, **162**, 1685–1691.

AJUEBOR, M.N., HOGABOAM, C.M., KUNKEL, S.L., PROUDFOOT, A.E.I. & WALLACE, J.L. (2001). The chemokine RANTES is a crucial mediator of the progression from acute to chronic colitis in the rat. *J. Immunol.*, **116**, 552–558.

ALAM, R., FORSYTHE, P.A., STAFFORD, S., LETT-BROWN, M.A. & GRANT, J.A. (1992). Macrophage inflammatory protein-1 alpha activates basophils and mast cells. *J. Exp. Med.*, **176**, 781–786.

APPLETON, I., TOMLINSON, A., COLVILE-NASH, P.R. & WILOUGH-BY, D.A. (1993). Temporal and spatial immunolocalization of cytokines in murine chronic granulomatous tissue. *Lab. Invest.*, **69**, 405–414.

BAGGIOLINI, M. (1998). Chemokines and leukocyte traffic. *Nature*, **392**, 562–568.

BAILEY, P.J., STURM, A. & LOPEZ-RAMOS, B. (1982). A biochemical study of the cotton pellet granuloma in the rat. Effects of dexamethasone and indomethacin. *Biochem. Pharmacol.*, **31**, 1213–1218.

CAROLLO, M., CHRISTIE, M. & PERRETTI, M. (1999). CC chemokine expression in a murine model of chronic granuloma. *Br. J. Pharmacol.*, **128**, 22P.

CAROLLO, M., CHRISTIE, M.I. & PERRETTI, M. (2000). Expression of MIP-2, KC and MCP-1 and their receptors in chronic granulomatous inflammation. *Br. J. Pharmacol.*, **131**, 168P.

CHENSUE, S.W., WARMINGTON, K.S., RUTH, J.H., SANGHI, P.S., LINCOLN, P. & KUNKEL, S.L. (1996). Role of monocyte chemoattractant protein-1 (MCP-1) in Th1 (Mycobacterial) and Th2 (Schistosomal) antigen-induced granuloma formation. *J. Immunol.*, **157**, 4602–4608.

COLVILLE-NASH, P.R., ALAM, C.A.S., APPLETON, I., BROWN, J.R. & SEED, M.P. (1995). The pharmacological modulation of angio-genesis in chronic granulomatous infammation. *J. Pharmacol. Exp. Ther.*, **274**, 1463–1472.

DALLEGRI, F. & OTTONELLO, L. (1997). Tissue injury in neutrophilic inflammation. *Inflamm. Res.*, **46**, 382–391.

DE MOULDER, P.H., VAN RENNES, H., MIER, P.D., BERGERS, M., DE PAUW, B.E. & HAANEN, C. (1983). Characterisation of monocyte maturation in adherent and suspension cultures and its application to study monocyte differentiation in Hodgkin's disease. *Clin. Exp. Immunol.* **54**, 681–688.

DI PIETRO, A., BURDICK, M., LOW, Q.E., KUNKEL, S.L. & STRIETER, R.M. (1998). MIP-1α as a critical macrophage chemoattractant in murine wound repair. *J. Clin. Invest.*, **101**, 1693–1698.

FURIE, M.B. & RANDOLPH, G.J. (1995). Chemokines and tissue injury. *Am. J. Pathol.*, **146**, 1287–1301.

GAO, J.-L., WYNN, T.A., CHANG, Y., LEE, E.J., BROXMEYER, H.E., COOPER, S., TIFFANY, H.L., WESTPHAL, H., KWON-CHUNG, J. & MURPHY, P.M. (1997). Impaired host defense, hematopoiesis, granulomatous inflammation and type 1-type 2 cytokine balance in mice lacking CC chemokine receptor 1. *J. Exp. Med.*, **185**, 1959–1968.

GIBSON, U.E.M., HEID, C.A. & WILLIAMS, P.M. (1996). A novel method for real time quantitative RT-PCR. *Genome Res.*, **6**, 995–1001.

GRANGER, D.N. & KUBES, P. (1994). The microcirculation and inflammation: modulation of leukocyte- endothelial cell adhe-sion. *J. Leukoc. Biol.*, **55**, 662–675.

HARRIS, J.G., FLOWER, R.J., WATANABE, K., TSURUFUJI, S., WOLITZKY, B.A. & PERRETTI, M. (1996). Relative contribution of the selectins in the neutrophil recruitment caused by the chemokine cytokine induced neutrophil chemoattractant (CINC). *Biochem. Biophys. Res. Comm.*, **221**, 692–696.

HEID, C.A., STEVENS, J., LIVAK, K.J. & WILLIAMS, P.M. (1996). Real time quantitative PCR. *Genome Res.*, **6**, 986–994.

HIRAYAMA, Y., SAKAMAKI, S., MATSUNAGA, T., KUGA, T., KURODA, H., KUSAKABE, T., SASAKI, K., FUJIKAWA, K., KATO, J., KOGAWA, K., KOYAMA, R. & NIITSU, Y. (1998). Concentra-tions of thrombopoietin in bone marrow in normal subjects and in patients with idiopathic thrombocytopenic purpura, aplastic anemia, and essential thrombocythemia correlate with its mRNA expression of bone marrow stromal cells. *Blood*, **92**, 46–52.

HOGABOAM, C.M., BONE-LARSON, C.L., LIPINSKI, S., LUKACS, N.W., CHESUE, S.W., STRIETER, R.M. & KUNKEL, S.L. (1999). Differential monocyte chemoattractant protein-1 and chemokine receptor 2 expression by murine lung fibroblasts derived from Th1- and Th2-type pulmonary granuloma models. *J. Immunol.*, **163**, 2193–2201.

JOHNSTON, B., BURNS, A.R., SUEMATSU, M., ISSEKUTZ, T.B., WOODMAN, R.C. & KUBES, P. (1999). Chronic inflammation upregulates chemokine receptors and induces neutrophil migra-tion to monocyte chemoattractant protein-1. *J. Clin. Invest.*, **103**, 1269–1276.

KASAMA, T., STRIETER, R.M., LUKACS, N.W., LINCOLN, P.M. & BURDICK, M.D. (1995). Interleukin-10 expression and chemo-kine regulation during the evolution of murine type II collagen-induced arthritis. *J. Clin. Invest.*, **95**, 2868–2876.

KIMURA, M., SUZUKI, J. & AMEMIYA, K. (1985). Mouse granuloma pouch induced by Freund's complete adjuvant with croton oil. *J. Pharmacobio-Dyn.*, **8**, 393–400.

KIMURA, M., AMEMIYA, K., YAMADA, T. & SUZUKI, J. (1986). Quantitative method for measuring adjuvant-induced granuloma amgiogenesis in insulin-treated diabetic mice. *J. Pharmacobio-Dyn.*, **9**, 442–446.

KOCH, A.E., KUNKEL, S.L., SHAH, M.R., HOSAKA, S., HALLORAN, M.M., HAINES, G.K., BURDICK, M.D., POPE, R.M. & STRIETER, R.M. (1995). Growth-related gene product α. *J. Immunol.*, **155**, 3660–3666.

KORTHUIS, R.J., ANDERSON, D.C. & GRANGER, D.N. (1994). Role of neutrophilendothelial cell adhesion in inflammatory disorders. *J. Crit. Care*, **9**, 47–71.

KUNKEL, S.L., CHENSUE, S.W., STRIETER, S.M., LYNCH, J.P. & REMICK, D.G. (1989). Cellular and molecular aspects of granulomatous inflammation. *Am. J. Respir. Cell Mol. Biol.*, **1**, 439–447.

KUNKEL, S.L., LUKACS, N., KASAMA, T. & STRIETER, R.M. (1996). The role of chemokines in inflammatory joint disease. *J. Leukoc. Biol.*, **59**, 6–12.

LIE, Y.S. & PETROPOULOS, C.J. (1998). Advances in quantitative PCR technology: 5′ nuclease assays. *Curr. Opin. Biotech.*, **9**, 43–48.

LLOYD, C.M., MINTO, A.W., DORF, M.E., PRODUFOOT, A., WELLS, T.N., SALANT, D.J. & GUTIERREZ-RAMOS, J.C. (1997). RANTES and monocyte chemoattractant protein-1 (MCP-1) play an important role in the inflammatory phase of crescentic nephritis, but only MCP-1 is involved in crescent formation and interstitial fibrosis. *J. Exp. Med.*, **185**, 1371–1378.

LUSTER, A.D. (1998). Chemokines – Chemotactic cytokines that mediate inflammation. *New Engl. J. Med.*, **12**, 436–445.

MANTOVANI, A. (1999). The chemokine system: redundancy for robust outputs. *Immunol. Today*, **20**, 254–257.

MARQUEZ, L.A. & DUNFORD, B. (1997). Mechanism of the oxidation of 3,5,3′,5′-tetramethylbenzidine by myeloperoxidase determined by transient- and steady-state kinetics. *Biochemistry*, **36**, 9349–9355.

MULLANE, K.M., KRAEMER, R. & SMITH, B. (1985). Myeloperoxidase activity as a quantitative assessment of neutrophil infiltration into ischemic myocardium. *J. Pharmacol. Meth.*, **14**, 157–163.

MURPHY, P.M., BAGGIOLINI, M., CHARO, I.F., HEBERT, C.A., HORUK, R., MATSUSHIMA, K., MILLER, L.H., OPPENHEIM, J.J. & POWER, C.A. (2000). International Union of Pharmacology. XXII. Nomenclature for chemokine receptors. *Pharmacol. Rev.*, **52**, 145–176.

MURPHY, W.J., TIAN, Z.-G., ASAI, O., FUNAKOSHI, S., ROTTER, P., HENRY, M., STRIETER, R.M., KUNKEL, S.L., LONGO, D.L. & TAUB, D.D. (1996). Chemokines and T lymphocyte activation. II. Facillitation of human T cell trafficking in severe combined immunodeficiency mice. *J. Immunol.*, **156**, 2104–2111.

ORLANDO, C., PINZANI, P. & PAZZAGLI, M. (1998). Developments in quantitative PCR. *Clin. Chem. Lab. Med.*, **36**, 255–269.

PAUL, W.E. & SEDER, R.A. (1994). Lymphocyte responses and cytokines. *Cell*, **76**, 241–251.

PREMACK, B.A. & SCHALL, T.J. (1996). Chemokine receptors: gateways to inflammation and infection. *Nature Med.*, **2**, 1174–1178.

ROVAI, L.E., HERSCHMAN, H.R. & SMITH, J.B. (1998). The murine neutrophilchemoattractant chemokines LIX, KC, and MIP-2 have a distinct induction kinetic, tissue distributions, and tissue-specific sensitivities to glucocorticoid regulation in endotoxemia. *J. Leukoc. Biol.*, **64**, 494–562.

SMITH, R.E., HOGABOAM, C.M., STRIETER, R.M., LUKACS, N.W. & KUNKEL, S.L. (1997). Cell-to-cell and cell-to-matrix interactions mediate chemokine expression: an important component of the inflammatory lesion. *J. Leukoc. Biol.*, **62**, 612–619.

STANDIFORD, T.J., ROLFE, M.W., KUNKEL, S.L., LYNCH, III, J.P., BURDICK, M.D., GIBERT, A.R., ORRINGER, M.B., WHYTE, R.I. & STRIETER, R.M. (1993). Macrophage inflammatory protein-1 α expression in interstitial lung disease. *J. Immunol.*, **151**, 2852–2863.

STANDIFORD, T.J., STRIETER, R.M., LUKACS, N.W. & KUNKEL, S.L. (1995). Neutralisation of IL-10 increases lethality in endotoxemia. Cooperative effects of macrophage inflammatory protein-2 and tumor necrosis factor. *J. Immunol.*, **155**, 2222–2229.

TAILOR, A., TOMLINSON, A., SALAS, A., PANÉS, J., GRANGER, D.N., FLOWER, R.J. & PERRETTI, M. (1999). Dexamethasone inhibition of leukocyte adhesion to rat mesenteric postcapillary venules: role of intercellular adhesion molecule 1 and KC. *Gut*, **45**, 705–712.

THORNTON, S., DUWEL, L.E., BOIVIN, G.P., MA, Y. & HIRSCH, R. (1999). Association of the course of collagen-induced arthritis with distinct patterns of cytokine and chemokine messanger RNA expression. *Arth. Rheum.*, **42**, 1109–1118.

WARD, P. (1997). Neutrophils and adjuvant arthritis. *Clin. Exp. Immunol.*, **107**, 225–226.

ZISMAN, D.A., KUNKEL, S.L., STRIETER, R.M., TSAI, W.C., BUCKNELL, K., WILKOWSKI, J. & STANDIFORD, T.J. (1997). MCP-1 protects mice from lethal endotoxemia. *J. Clin. Invest.*, **99**, 2832–2836.

ZLOTNIK, A. & YOSHIE, O. (2000). Chemokines: a new classification system and their role in immunity. *Immunity*, **12**, 121–127.